Nanoscale

COMMUNICATION

View Article Online
View Journal | View Issue

Cite this: *Nanoscale*, 2016, **8**, 3906

Received 1st December 2015,
Accepted 22nd January 2016

DOI: 10.1039/c5nr08509h

www.rsc.org/nanoscale

Gas-phase rapid reduction of graphene oxide through photoionization of gold nanoparticles†

Jeong Hoon Byeon*

This work introduces for the first time the rapid reduction of graphene oxide *via* the photoionization of gold nanoparticles in a continuous gas-phase process. Ejected electrons from gold nanoparticles facilitated the rapid photoinduced reduction of GO nanoflakes without the use of wet chemical processes.

Graphene [*i.e.* reduced graphene oxide (rGO)] has attracted much interest for its unique physical and chemical properties and wide-ranging technological applications,[1–3] such as for electronic devices, batteries, solar energy conversion, catalysis, *etc*.[4] The first challenge is to process graphene sheets for their use in practical applications. Many methods have been developed to fabricate graphene materials, including micromechanical exfoliation, chemical vapor deposition, the reduction of GO, *etc*.[5–7] Among these methods, chemical reduction is considered to be the most effective and economical way of preparing rGO from GO. However, chemical reduction usually requires toxic chemicals, several tedious batch steps, high temperatures and energies, and special instruments and controls for the preparation of rGO, which limit its practical applications.[1,8] Thus, the development of an environmentally friendly preparation strategy is highly desired.

Extensive research studies have focused on the construction of graphene-based hybrid nanomaterials because these materials not only combine the merits of each component, but also offer the potential to introduce new properties that can potentially be used in a diverse range of applications.[9] Indeed, considerable effort has been devoted to fabricating binary materials of graphene as a 2D scaffold and metallic, semiconductor, or photoactive materials as a viable alternative to boost the efficiency of various catalytic and storage reactions in energy conversion applications.[10] More recently, interest has centered on hybrid materials based on gold (Au) nanoparticles, and as a result, the deposition of Au nanoparticles onto material surfaces has been extensively investigated for the novel interparticle properties of Au nanoparticles in catalysis, sensing, for biomaterials, as well as in electronic and optoelectronic devices.[11] The incorporation of Au nanoparticles onto material surfaces often requires preparing a specific functionality on the Au nanoparticles and pretreatment of the material surfaces to find suitable reaction partners for the assembly of the hybrid materials,[12] and thus it is still a challenge to prepare the Au/rGO hybrid materials in a simple, green, and continuous synthesis manner.

Nanometer-sized (<several tens of nanometers) graphene sheets have recently received much attention, especially in relation to cellular imaging and drug delivery[13] because of their size-matching interface with biological systems and the high stability of graphene in an aqueous environment. The present work introduces a rapid gas-phase reduction of GO nanoflakes, and to the best of our knowledge, this is the first attempt to reduce GO nanoflakes *via* photoionization of Au nanoparticles. As shown in Scheme 1 (details are also given in

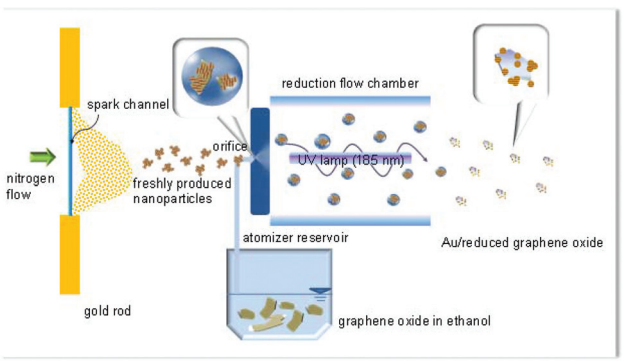

Scheme 1 Continuous gas-phase reduction of GO *via* the photoionization of Au nanoparticles. Spark produced Au nanoparticles were incorporated with nanoscale GO flakes as a form of Au/GO, and the GO flakes were then reduced by electrons from photoionized Au particles in a single-pass configuration.

School of Mechanical Engineering, Yeungnam University, Gyeongsan 38541, Republic of Korea. E-mail: postjb@yu.ac.kr; Tel: +82 53 810 2451

†Electronic supplementary information (ESI) available: The experimental details, TEM images of graphite nanoparticles, and Raman and XPS spectra of GO and rGO. See DOI: 10.1039/c5nr08509h

the ESI†), freshly spark-produced Au nanoparticles, and the particle-laden flow passed over the collison atomizer orifice where they mixed with the atomized GO (from graphite nanoparticles shown in Fig. S1, ESI†) solution to form hybrid droplets. The droplets then passed through a UV (UVP, USA) irradiation chamber to ionize Au nanoparticles, resulting in Au/rGO hybrid nanoflakes.

To prepare fresh Au nanoparticles, first, a spark discharge in a nitrogen environment was employed. The gas temperature inside the spark channel was increased beyond a critical value, which was sufficient to sublimate parts of the Au electrodes.[14] The duration of each spark was very short (~1 ms) and the vapors cooled rapidly downstream of the spark. This formed a supersaturation resulting in particle formation through nucleation–condensation. The total number concentration (TNC), geometric mean diameter (GMD), and geometric standard deviation (GSD) of the Au particles, which were measured using a scanning mobility particle sizer (3936, TSI, USA), were 8.32×10^6 particles per cm^3, 24.0 nm, and 1.50, respectively, as shown in Fig. 1a. According to gravimetric measurements, the energy required to produce 1 g of Au particles was of the order of 10^6 J. Au/GO hybrid nanoflakes were formed by incorporating Au with GO during the collison atomization of the GO solution (GO suspended in ethanol). We verified the incorporation of the Au nanoparticles with GO nanoflakes by measuring the size distributions of the GO and Au/GO flakes in the gas-phase. The GMD, GSD, and TNC of the Au/GO hybrid flakes were 3.90×10^6 particles per cm^3, 30.0 nm, and 1.61, respectively. The analogous data for GO were 2.74×10^6 cm^{-3}, 30.7 nm, and 1.57, respectively. The size distribution of the Au/GO was rather similar to the GO flakes compared to that of the Au particles, and there was no bimodal distribution character, implying that the Au particles were nearly quantitatively incorporated with the GO to form Au/GO hybrid flakes. UV-vis spectroscopy provided further characterization of the incorporation between the Au particles and the GO flakes (Fig. 1b). A surface plasmon resonance band was centered at 530 nm, which is characteristic of Au nanoparticles. The spectrum of GO shows a shoulder at 240 nm, corresponding to the $\pi \rightarrow \pi^*$ transitions of aromatic C=C bonds and the $n \rightarrow \pi^*$ transitions of C=O bonds.[15] As can be observed, the UV-vis absorption of the Au/GO hybrid flakes shows a weak shoulder at 270 nm and a broad growing peak at ~500 nm, indicating the presence of the Au nanoparticles in the Au/GO hybrid flakes.

Low and high magnification transmission electron microscopy (TEM, JEM-3010, JEOL, Japan) images show the morphology of the Au, GO, Au/GO, and Au/rGO samples. Specimens were prepared for examination in the TEM by direct electrostatic gas-phase sampling at a sampling flow of 1.0 L min^{-1} and an operating voltage of 5 kV using a Nano Particle Collector (NPC-10, HCT, Korea). The TEM images for Au reveal that the Au nanoparticles were agglomerates of several primary particles (each ~3 nm in diameter) with lattice fringes of 0.23 nm corresponding to the (111) plane. The morphology of the GO was as flakes, and a high resolution image of the GO shows a regular hexagonal structure, as is expected for graphene, while several internal defects could also be found within the structure. When the Au particles passed over the orifice of the collison atomizer, most Au particles were attached to the GO flakes, resulting in Au/GO hybrid nanoflakes. Moreover, the Au particles were redistributed on the GO flakes due to deagglomeration (by setting the force acting on an agglomerate of size D_{pa} due to the sudden pressure change across an orifice in the collison atomizer), and the size is given by[16]

$$D_{pr} = \alpha\sqrt{\frac{D_{pa}H}{6\pi\Delta P\Theta^2}} \quad (1)$$

where D_{pr} is the size of a restructured agglomerate, α is the proportionality constant, H is the Hamaker constant, ΔP is the pressure difference between the front and the rear of the

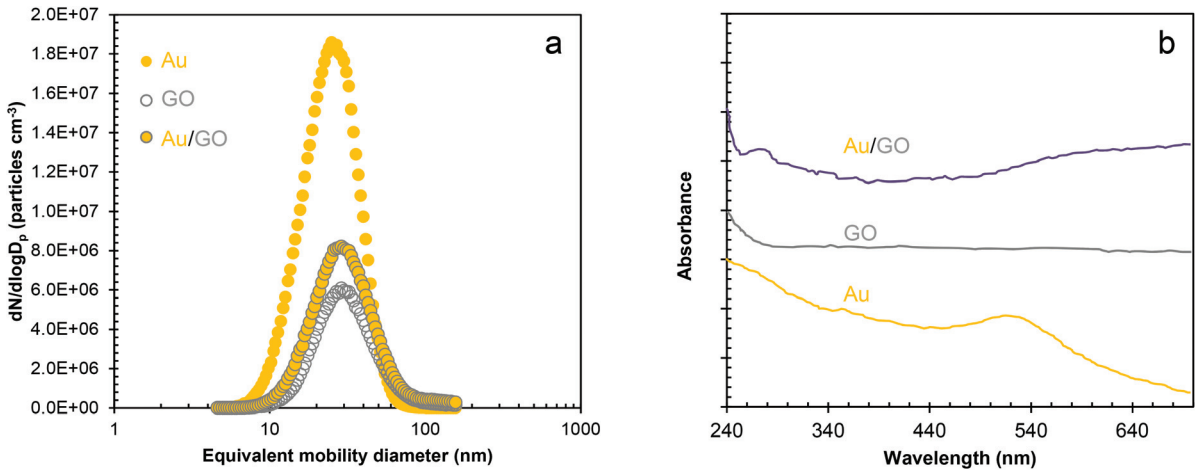

Fig. 1 Results of the incorporation of the Au nanoparticles with GO nanoflakes. (a) Size distributions of spark produced Au, collison atomized GO, and their incorporated nanostructures (Au/GO) in the gas-phase. (b) UV-vis spectra of the Au nanoparticles, GO nanoflakes, and Au/GO hybrid nanoflakes.

orifice, and Θ is the parameter controlling the maximum cohesive strength between the constituent particles in an agglomerate. Au agglomerates pass through the orifice, and the rapid changes in pressure, density, and velocity across the orifice produce an impulse capable of shattering the agglomerates. It seems that the incorporation between Au and GO inhibited a dislocation of Au from the GO during gas-phase synthesis. This is probably due to the capillary ($F_{cap} = 4\pi r_p \gamma \cos\theta$, where r_p, γ, and θ are the particle radius, surface tension, and contact angle between the Au and GO, respectively) and electrostatic attraction ($F_{ea} = \frac{1}{4\pi\varepsilon_0}\frac{q_1 q_2}{d^2}$, where ε_0 is the permittivity constant, d is the distance between the Au and GO, and q_1 and q_2 are surface charges of the Au and GO, respectively) forces between the Au and GO. Spark produced particles normally have positive charges owing to a photo- and/or electric-induced ionization of their surface during spark particle formation.[17] In addition, GO has negative charges from carboxylates on its structure.[18] Fig. 2 also shows the Au/GO hybrid nanoflakes after photoinduced reduction *via* electron ejections from ionized Au nanoparticles. There were no significant differences in the morphology before and after the reduction, but the distribution of the Au nanoparticles on a graphene flake probably changed due to different surface charge states of the Au particles.

Fig. 3 displays Fourier transform infrared (FTIR, IFS 66/S, Bruker Optics, Germany) spectra of GO and Au/rGO nanoflakes. GO exhibits broad IR peaks at around 3400 and 1730 cm^{-1} corresponding to the O–H stretching and C=C vibrations, respectively, and also shows carboxyl C=O (1780 cm^{-1}), and hydroxyl C–OH (1390 cm^{-1}) stretching vibrations of COOH groups. Au/rGO shows a featureless spectrum at the given absorbance scales, implying a reduction in the amount of oxygen functionalities (also verified using Raman spectroscopy (Fig. S2, ESI†)). X-ray photoelectron spectroscopy (XPS, K-Alpha, Thermo Scientific, USA) analyses were further employed to confirm the reduction of GO. Fig. S3 (ESI†) shows the C 1s spectra of GO and reduced GO samples. In the GO sample, the C 1s signals deconvoluted into several binding signals for C–C (284.5 eV), C–O (286.2 eV), C=O (287.8 eV), O–C=O (288.9 eV), and O–CO–O (290.8 eV). The fraction of C–C bonds (sp^2 carbon) increased from 0.604 to

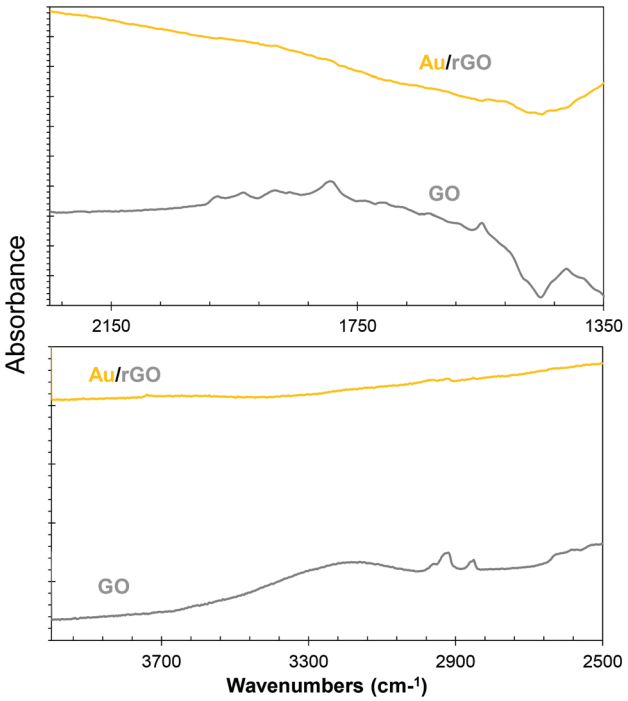

Fig. 3 FTIR spectra of the GO and Au/rGO (reduced GO nanoflakes *via* photoionization of Au nanoparticles) hybrid nanoflakes.

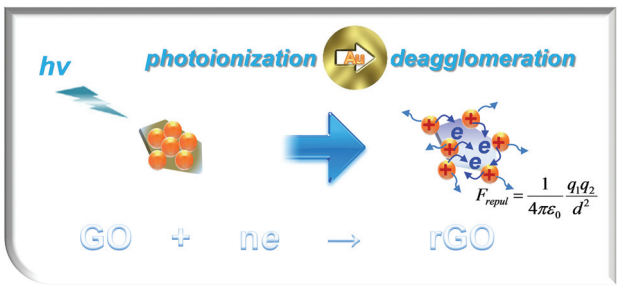

Scheme 2 Mechanism for the reduction of GO *via* the photoionization of Au nanoparticles. UV irradiation induces a redistribution in the surface charge of Au nanoparticles, which may reduce GO by electron transfer.

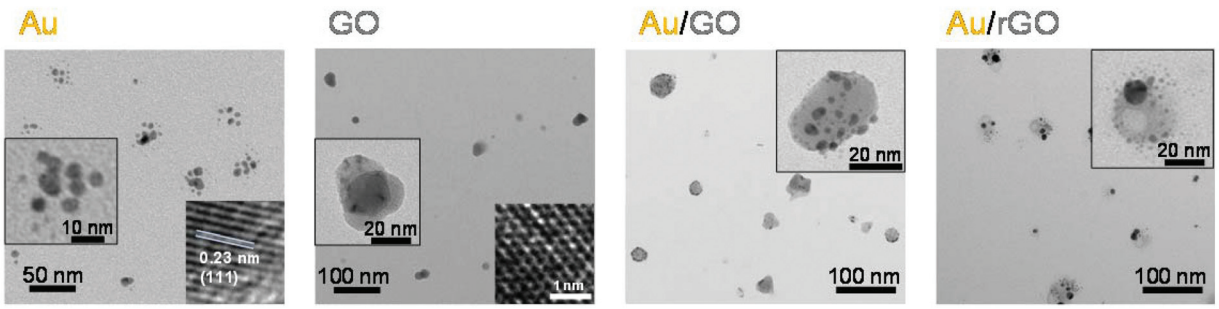

Fig. 2 TEM images of the Au nanoparticles, GO nanoflakes, and Au/GO and Au/rGO (reduced GO nanoflakes *via* photoionization of Au nanoparticles) hybrid nanoflakes.

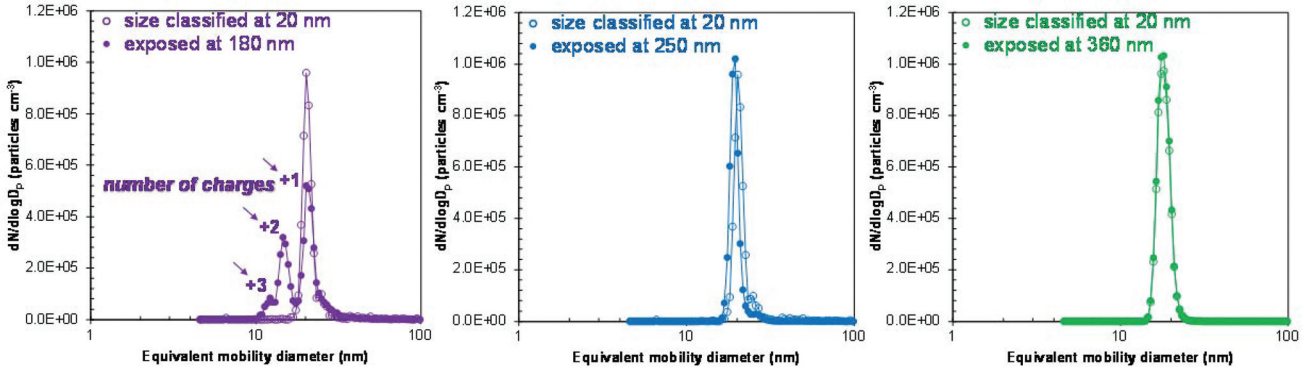

Fig. 4 Charge distributions of the Au nanoparticles under UV irradiation with wavelengths of 180, 250, and 360 nm.

0.855 *via* a photoionization process. The first step of the proposed mechanism (Scheme 2) shows the ejection of electrons during the photoionization of the Au nanoparticles on a GO flake. In step 2, released electrons were used to convert GO to rGO, a reduced form of GO. In addition, photo-induced OH radicals dissociated from ethanol molecules during the photoionization may also affect the reduction of GO flakes.[3,19]

To verify electron ejections from Au nanoparticles, we measured the charge distributions of Au nanoparticles after the photoionization process using a tandem differential mobility analyzer (DMA) system (details are given in the ESI†). Fig. 4 shows the charge distributions of photoionized gold particles with different UV wavelengths of 180, 250, and 300 nm. Different peaks appearing in the first image correspond to the different numbers of charges on the particles. The number of elementary charges q of the photoionized particles was estimated using the following equation:[20]

$$q = \frac{Z_{\mathrm{p,NDMA2}}}{Z_{\mathrm{p,NDMA1}}} \quad (2)$$

where $Z_{\mathrm{p,NDMA1}}$ and $Z_{\mathrm{p,NDMA2}}$ are the electrical mobilities measured by nanoDMA (NDMA, 3085, TSI, USA) 1 and 2, respectively. The results revealed that photoionization induced positive charges on the particles, and this implies that electrons were ejected from the Au nanoparticles which were being used to reduce the GO. On the other hand, photoionization from the other UV wavelengths (at 250 and 360 nm) did not induce electron ejections. The measured charge distributions at wavelengths of 250 and 360 nm coincided with their initial distributions before UV irradiation, and this implies that there was no significant reduction of GO *via* ejected electrons.

We developed for the first time a continuous gas-phase reduction of GO nanoflakes and the simultaneous fabrication of Au/rGO hybrid nanoflakes as a simple, green, and generalizable process, which have a self-assembled hybrid nanostructure. Most previous GO reductions employed a harsh and hazardous material-based treatment of micrometer-sized GO sheets. Because of the gas-phase photoionization of the Au nanoparticles, this platform facilitated the easy photoinduced reduction of the GO nanoflakes. The proposed method opens up a new way of obtaining rGO or graphene-based hybrid nanomaterials for a broad range of practical applications.

Acknowledgements

This work was supported by a National Research Foundation of Korea grant funded by the Korean Government (NRF-2015R1A2A2A04005809).

Notes and references

1 T. Wu, S. Liu, Y. Luo, W. Lu, L. Wang and X. Sun, *Nanoscale*, 2011, **3**, 2142.
2 Y. Pan, H. Bao and L. Li, *ACS Appl. Mater. Interfaces*, 2011, **3**, 4819.
3 Y. H. Ding, P. Zhang, Q. Zhuo, H. M. Ren, Z. M. Yang and Y. Jiang, *Nanotechnology*, 2011, **22**, 215601.
4 H. Li, S. Liu, J. Tian, L. Wang, W. Lu, Y. Luo, A. M. Asiri, A. O. Al-Youbi and X. Sun, *ChemCatChem*, 2012, **4**, 1079.
5 A. Zangwill and D. D. Vvedensky, *Nano Lett.*, 2011, **11**, 2092.
6 N. C. Bartelt and K. F. McCarty, *MRS Bull.*, 2012, **37**, 1158.
7 T. Kuila, A. K. Mishra, P. Khanra, N. H. Kim and J. H. Lee, *Nanoscale*, 2013, **5**, 52.
8 H. N. Lim, N. M. Huang and C. H. Loo, *J. Non-Cryst. Solids*, 2012, **358**, 525.
9 Z. Jin, D. Nackashi, W. Lu, C. Kittrell and J. M. Tour, *Chem. Mater.*, 2010, **22**, 5695.
10 P. V. Kamat, *J. Phys. Chem. Lett.*, 2011, **2**, 242.
11 H. Ismaili, D. Geng, A. X. Sun, T. T. Kantzas and M. S. Workentin, *Langmuir*, 2011, **27**, 13261.
12 M. L. Curri, R. Comparelli, M. Striccoli and A. Agostiano, *Phys. Chem. Chem. Phys.*, 2010, **12**, 11197.
13 X. Sun, Z. Liu, K. Welsher, J. T. Robinson, A. Goodwin, S. Zaric and H. Dai, *Nano Res.*, 2008, **1**, 203.

14 J. H. Byeon, J. H. Park and J. Hwang, *J. Aerosol Sci.*, 2008, **39**, 888.
15 T. A. Pham, B. C. Choi, K. T. Lim and Y. T. Jeong, *Appl. Surf. Sci.*, 2011, **257**, 3350.
16 J. H. Byeon and J. T. Roberts, *Chem. Mater.*, 2012, **24**, 3544.
17 J. H. Byeon and J.-W. Kim, *Langmuir*, 2010, **26**, 11928.
18 L. Guardia, S. Villar-Rodil, J. I. Paredes, R. Rozada, A. Martínez-Alonso and J. M. D. Tascón, *Carbon*, 2012, **50**, 1014.
19 C.-Y. Su, Y. Xu, W. Zhang, J. Zhao, A. Liu, X. Tang, C.-H. Tsai, Y. Huang and L.-J. Li, *ACS Nano*, 2010, **4**, 5285.
20 J. H. Byeon, J. H. Ji, J. H. Park, K. Y. Yoon and J. Hwang, *J. Aerosol Sci.*, 2008, **39**, 460.